RSC Advances

PAPER

View Article Online
View Journal | View Issue

Cite this: *RSC Adv.*, 2017, **7**, 9605

Fabrication of intracrystalline mesopores within zeolite Y with greatly decreased templates

Zhen Wang,[a] Honghai Liu,[b] Qingting Meng,[a] Junsu Jin,[a] Chunyan Xu,[a] Xiaotong Mi,[a] Xionghou Gao[b] and Hongtao Liu*[a]

Received 23rd October 2016
Accepted 17th January 2017

DOI: 10.1039/c6ra25698h

rsc.li/rsc-advances

Zeolite Y with intracrystalline mesopores has been emerging as one of the most potential materials in the catalytic cracking of large molecules. Our group has reported the synthesis of zeolite Y with intracrystalline mesopores with the formula $[(CH_3O)_3SiC_3H_6N(CH_3)_2C_{18}H_{37}]Cl$ (denoted as "TPOACl"). However, the fabrication of mesoporous zeolite Y with a decreased organic template remains a significant challenge. In this study, a novel surfactant $[(CH_3O)_3SiC_3H_6N(CH_3)_2C_{16}H_{33}]Cl$ (denoted as "TPHAC") was designed and synthesized using low-cost industrial raw materials, which was found suitable for the formation of mesoporosity utilizing greatly decreased amount of the surfactant. The possible differences in the synthesis mechanisms of TPOACl and TPHAC have been discussed. The enhanced hydrophilicity of the hydroxyl groups and the subsequent decrease in the micelle aggregation number (MAN) are proposed to be the key to underline the decreased amount of surfactant in the successful synthesis. The material shows excellent hydrothermal stability and a higher mesoporous surface area ratio than TPOACl. The prepared mesoporous zeolite Y showed much higher catalytic activity and selectivity in heavy oil cracking than that prepared from TPOACl.

Introduction

Zeolite Y with intracrystalline mesopores has been widely applied in the processing of large molecules, such as in heavy oil catalytic cracking,[1,2] due to its high surface area, hydrothermal stability, and interconnected meso–micropores.[3–6] During the past few decades, intensive efforts have been devoted to the synthesis of hierarchical zeolite such as Y, ZSM-5, and beta.[7–12]

Typical ways to introduce mesopores into Y and ZSM-5 are post-synthetic dealumination or desilication treatments.[13–16] However, these methods lead to the partial crystal collapse of intact zeolite. Another recognized route is adopting a hard template such as carbon materials[17] or nanotubes.[18] Unfortunately, a complicated procedure is required to improve the compatibility between the hard templates and inorganic species, which is not suitable for scale-up production. Therefore, one effective solution to this problem is to explore a novel template that can be anchored into the aluminosilicate gel of raw materials. Ryoo *et al.*[19] reported that crystalline zeolites with tunable mesoporosity were synthesized using amphiphilic organosilanes. Note that this approach allows the highest versatility in controlling the mesoporosity in zeolite. Furthermore, the combining force between the templates and inorganic species was strong and phase separation was avoidable.[20] With this idea in mind, the authors of the present investigation introduced intracrystalline mesopores into zeolite Y and ZSM-5 with amphiphilic surfactants including TPOACl.[21,22] Moreover, the samples showed superior catalytic cracking properties when used in heavy oil processing. However, one key problem remains unresolved with respect to the synthesis of mesoporous Y: the synthesis cost is high due to a large amount of organic template, which limits their application in industrial processes. Therefore, the development of a novel template that can reduce the amount of organic surfactant required for the synthesis of mesoporous Y remains a challenging goal.

Generally, the hydrophobic alkyl chain could self-assemble to form micelles in water above the critical micelle concentration (CMC). The MAN gradually increases with the increasing length of the hydrophobic alkyl chain. The synthesis mechanism for mesoporous zeolites using amphiphilic organosilanes has been well explained with respect to ZSM-5 zeolite by Ryoo's group.[23] However, the effect of the tail length of the organosilane surfactants on the physicochemical properties of the resulting mesoporous zeolite has not yet been investigated. On this basis, we were inspired to attempt to reduce the amount of organic surfactant required for this reaction by decreasing the length of the hydrophobic alkyl chains.

Herein, we demonstrate for the first time the direct synthesis of TPHAC from *N*,*N*-dimethylhexadecylamine ($(CH_3)_2NC_{16}H_{33}$)

[a]*State Key Laboratory of Chemical Resource Engineering, Beijing University of Chemical Technology, Beijing 100029, P. R. China. E-mail: liuht@mail.buct.edu.cn; Tel: +86-1064448327*

[b]*Petrochemical Research Institute, Petrochina Company Limited, Beijing 100195, P. R. China*

and 3-chloropropyltrimethoxysilane ($(CH_3O)_3SiC_3H_6Cl$) *via* a condensation reaction followed by an *in situ* crystallization of mesoporous Y using industrial raw materials. In this strategy, TPHAC is firstly synthesized by the conventional route and introduced into the alkaline system as a mesoporogen for the synthesis of mesoporous zeolite Y. The MAN of TPHAC decreased significantly due to the reduced number of carbon atoms in the hydrophobic chains. Therefore, the amount of organic surfactant required was also significantly reduced by the employment of TPHAC. This one-pot strategy provides a facile approach for the synthesis of mesoporous Y with a considerably decreased cost, and this can potentially be used in the industrial processing of heavy oil cracking.

Experimental

Synthesis of mesoporous Y

TPHAC was synthesized according to the method described in the literature[24] and obtained as a 50 wt% solution in ethanol without purification. The synthesis procedures for mesoporous zeolite Y using TPHAC as a mesopore template are as follows: 6.5 g of initiator (with molar composition $16Na_2O/Al_2O_3/15SiO_2/320H_2O$) was added dropwise to 22.4 g water glass. An appropriate amount of TPHAC was added to the above solution under stirring. $Al_2(SO_4)_3$ and $NaAlO_2$ were added to the mixture under stirring for 1 h, resulting in a mixture with the molar composition: $Al_2O_3/SiO_2/Na_2O/H_2O/TPHAC = 12.5/100/62.5/2500/n$ (n = 2, 3, 4, and 5). The mixture was hydrothermally treated at 100 °C for 24 h. The crystallization products were collected by filtration, dried in air, and calcined at 550 °C for 5 h to remove the template. The obtained samples were designated as MY-x (x is the molar ratio of TPHAC/SiO_2).

For comparison, mesoporous NaY was synthesized by using TPOACl as a template according to the literature[21] with the molar composition: $Al_2O_3/SiO_2/Na_2O/H_2O/TPHACl = 12.5/100/62.5/2500/n$ (n = 2, 3, 4, and 5). The obtained samples were designated as MY-*a*, MY-*b*, MY-*c*, and MY-*d* with TPOACl/SiO_2 molar ratios of 0.02, 0.03, 0.04, and 0.05, respectively.

Conventional NaY (denoted as "classical NaY") was also synthesized according to our previous article.[21] Moreover, classical NaY was employed in this study as a reference zeolite.

Ion-exchange of mesoporous Y

The as-synthesized MY-0.03 was ion-exchanged twice with aqueous NH_4Cl (1 M) at 90 °C for 1 h, filtered, and washed thoroughly with deionized water before calcining at 550 °C for 2 h. The obtained protonic mesoporous form was designated as MHY-0.03. NaY was ion-exchanged using the above procedure and the product was designated as HY.

Characterization

N_2 adsorption–desorption measurements of the support and corresponding catalysts were performed on a Micromeritics ASAP 2420 instrument (USA). The specific surface areas were calculated using the Brunauer–Emmett–Teller (BET) method and the pore size distributions were obtained using the Barret–Joyner–Halenda (BJH) method. The samples to be measured were firstly degassed in a preparation station at 350 °C for 10 h and then switched to an analysis station for adsorption–desorption experiments at −196 °C. X-ray diffraction (XRD) experiments were performed on a Bruker D8 Advance diffractometer equipped with Cu Kα radiation (wavelength 1.5406°) with a working voltage of 40 kV and a current of 40 mA. XRD patterns were collected with a 2θ range between 5° and 45° and a scanning rate of 2° min^{-1}. The morphology of the synthesized zeolite was investigated with a HITACHI S4700 scanning electron microscope (SEM). Transmission electron microscopy (TEM) images were recorded with a JEOL JEM-3010 instrument with an accelerating voltage of 200 kV. All samples subjected to TEM measurements were ultrasonically dispersed in ethanol and dropped on the microgrid.

Catalytic cracking performance tests

Cat-1 was prepared from kaolin (65%), alumina gel (10%), and MHY-0.03 (25%); Cat-2 was prepared from kaolin (65%), alumina gel (10%), and HY (25%); Cat-3 was prepared from kaolin (65%), alumina gel (10%), and MHY-*c* (25%).[21] All the catalysts were crushed, sieved to 60–100 μm, and steamed in water vapor at 800 °C before use. Heavy oil catalytic cracking tests were carried out in a microactivity unit.

Results and discussion

Effect of hydrophobic chains on amount of surfactant

The surfactant consists of hydrophobic carboxylic chains and hydrophilic groups. The hydrophobic chain ($-C_{18}H_{37}$ in TPOACl and $-C_{16}H_{33}$ in TPHAC) tends to clump together to form micelles and template the formation of mesopores. Compared with TPOACl, the hydrophobicity of the TPHAC surfactant weakens as the carbon number of the carboxylic chains decreases. This change would lead to a decrease in the MAN as well as in the size of the micelles.[24] As a result, a large number of integrated micelles will be obtained at the same molar ratio as TPHAC/SiO_2. This phenomenon is explained in Scheme 1.

In the present investigation, the utilization of TPHAC is 3 g zeolite per g TPHAC, which is 1.8 times that of TPOACl (1.67 g zeolite per g TPOACl). The advantage of the TPHAC route is

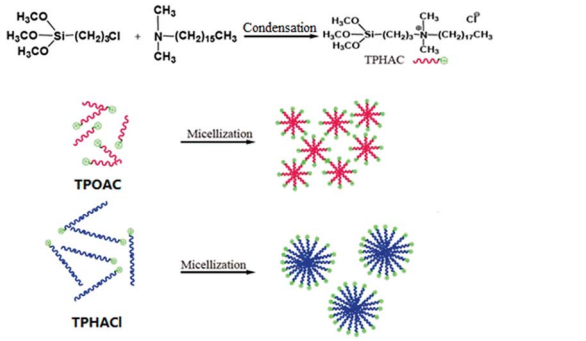

Scheme 1 The different mechanisms with TPOACl and TPHAC in the synthesis of MYs.

obvious: the preparation cost of mesoporous zeolite Y is reduced greatly; this has been an issue for researchers of mesoporous zeolites for a long time.

Factors affecting the fabrication of the mesophase and NaY crystallization

The influence of the amount of TPHAC on the physicochemical properties of MYs is studied. As shown in Fig. 1, all MYs show a typical IV isotherm with a H4 hysteresis loop above $P/P_0 = 0.5$, which is attributed to the capillary condensation of N_2 gas in the mesopores[25,26] and indicates the presence of mesoporous structures in the MY samples. The physicochemical properties of the MYs are listed in Table 1. Compared with the classical NaY (with a total surface area of 755 $m^2\ g^{-1}$),[21] the total surface areas of all the MYs showed a decrease (from 712 $m^2\ g^{-1}$ for MY-0.02 to 559 $m^2\ g^{-1}$ for MY-0.05). However, the surface area of the mesopores increased (from 84 $m^2\ g^{-1}$ for MY-0.02 to 179 $m^2\ g^{-1}$ for MY-0.05) as the amount of TPHAC increased. These results are fully consistent with those for mesoporous Y obtained with TPOACl by the authors of the present investigation.[21]

Interestingly, with the same template/SiO_2 molar ratio, the S_{meso}/S_{micro} and V_{meso}/V_{micro} ratios were found to have increased with TPHAC as compared to with TPOACl.[21] Compared with the Fu's report,[6] mesoporous Y was synthesized using TPOAB as mesoprogen with the TPOAB/SiO_2 molar ratio = 0.04, and the mesoporous surface area in this case was lower than that of MY-0.04. The influence of the surfactant on the physicochemical properties of the MYs can be essentially attributed to the micelles. A larger amount of micelles will be formed in the TPHAC system due to the decreased MAN, which will enhance the mesoporous surface area.

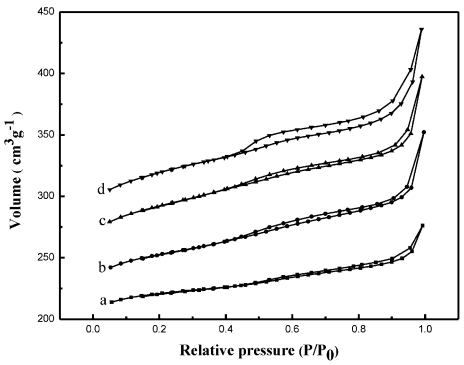

Fig. 1 Nitrogen adsorption–desorption isotherms of (a) MY-0.02, (b) MY-0.03, (c) MY-0.04, and (d) MY-0.05.

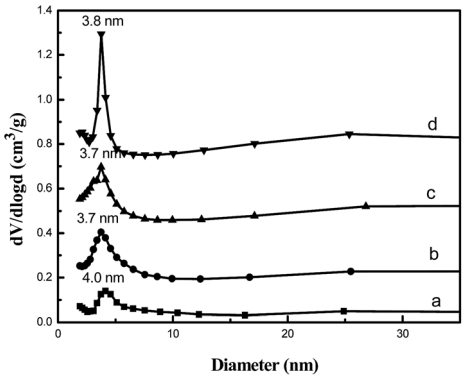

Fig. 2 BJH pore size distribution curves of (a) MY-0.02, (b) MY-0.03, (c) MY-0.04, and (d) MY-0.05.

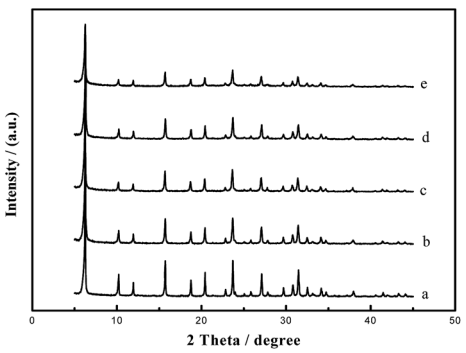

Fig. 3 XRD patterns of (a) classical NaY, (b) MY-0.02, (c) MY-0.03, (d) MY-0.04, and (e) MY-0.05.

In addition, the pore size was reduced in the TPHAC system (to about 4 nm) implying a decreased micelle size under the same molar ratio of surfactant/SiO_2. The pore size distribution curves of the MYs in the present investigation exhibit relatively uniform mesopore distributions with the predominant distribution concentered at about 4 nm can be seen from Fig. 2 (the pore size distributions of the mesopore diameters were

Table 1 Physicochemical properties of the MYs

Samples	S_{BET} ($m^2\ g^{-1}$)	S_{mic} ($m^2\ g^{-1}$)	S_{meso} ($m^2\ g^{-1}$)	V_{total} ($cm^3\ g^{-1}$)	V_{mic} ($cm^3\ g^{-1}$)	V_{meso} ($cm^3\ g^{-1}$)	V_{meso}/V_{micro}	S_{meso}/S_{micro}	The relative crystallinity
MY-0.02	712	628	84	0.43	0.30	0.13	0.43	0.13	89%
MY-0.03	660	527	133	0.47	0.26	0.21	0.81	0.25	85%
MY-0.04	663	498	165	0.48	0.24	0.24	1.00	0.33	84%
MY-0.05	559	380	179	0.44	0.18	0.26	1.44	0.47	80%
MY-*a*[21]	638	562	76	0.48	0.30	0.18	0.60	0.14	—
MY-*b*[21]	650	563	87	0.53	0.30	0.23	0.77	0.15	—
MY-*c*[21]	696	551	145	0.59	0.30	0.29	0.97	0.26	—
MY-*d*[21]	601	475	126	0.49	0.23	0.26	1.13	0.27	—
Meso-Y[6]	n.a.	n.a.	137	—	—	n.a.	—	—	—

calculated *via* the (BJH) algorithm using the adsorption branch). It is generally accepted that the mesopore size distribution is dependent on the assembly state of the TPHAC moieties.[22] It is reported that the diameter of a TPHAC micelle is 4 nm.[24]

On the other hand, from Fig. 3 and Table 1, we can see that addition of TPHAC will affect the crystallization of zeolite NaY. Increasing the amount of TPHAC leads to a decreased crystallinity in the resultant NaY. These results are fully consistent with those of BET analyses.

Hydrothermal stability and catalytic properties

MY-0.03 with a typical meso/microporous structure was chosen as an example for characterization of its structure, hydrothermal stability, and catalytic properties. The TEM image (Fig. 4b) reveals a worm-like mesoporous structure and a well crystallized microphase. Fig. 4a is a corresponding SEM image. A *d*-spacing of 0.35 nm calculated from Fig. 4 is fully consistent with the XRD results (2θ reflections).

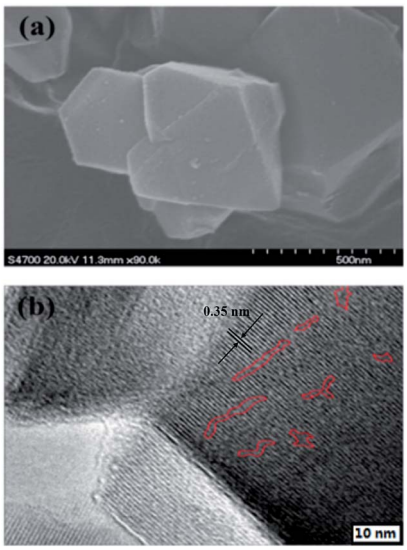

Fig. 4 (a) SEM images and (b) TEM images of MY-0.03.

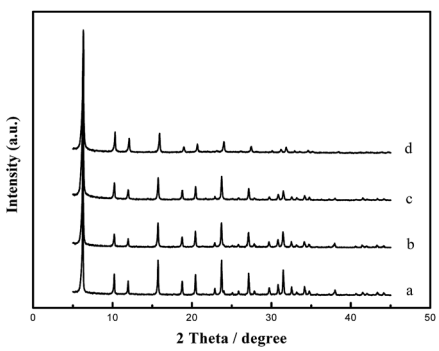

Fig. 5 XRD patterns of (a) classical NaY, (b) MY-0.03, (c) MHY-0.03, and (d) MHY-HT.

To evaluate the hydrothermal stability of the mesoporous Y, MHY-0.03 was hydrothermally treated in 100% water vapor for 4 h at 800 °C (the sample was denoted as MHY-HT). The XRD patterns of MY-0.03, MHY-0.03, and MHY-HT are shown in Fig. 5. As shown in Fig. 5, MHY-HT shows the major characteristic peaks of the (111), (331), (333), (533), (642), (660), and (555) planes. Moreover, the relative crystallinities of MHY-0.03 and MHY-HT were 76% and 47%, respectively, indicating the high hydrothermal stability of MY-0.03. Fig. 6 shows the TEM images of MHY-HT after hydrothermal treatment for 4 h. It can be seen that after the hydrothermal treatment, the intracrystalline mesopores were still present within the crystals. These results indicated that mesoporous Y obtained with as-synthesized TPHAC has excellent hydrothermal stability.

To evaluate the catalytic properties of zeolites obtained in the present investigation, three catalysts (Cat-1, Cat-2, and Cat-3), MHY-0.03, HY, and MHY-*c*[16] were selected and tested with Daqing heavy oil catalytic cracking as a model reaction system. From Table 2, it is clear that the yield of the light fraction (gasoline + diesel) with Cat-1 is 59.2 wt%, which is higher than that with Cat-2 (55.6 wt%). In addition to this, the yields of heavy oil and coke are lower than those with Cat-2. These results confirmed that the properties of the catalysts depended on the characteristics of the zeolites.

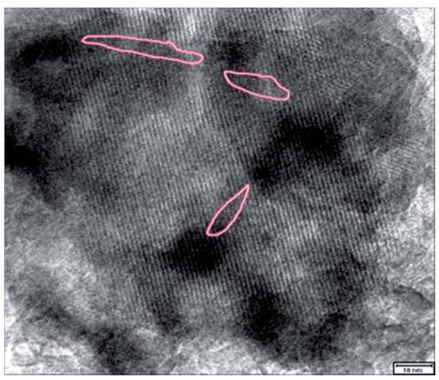

Fig. 6 TEM image of MHY-HT.

Table 2 Heavy oil catalytic cracking results

Catalyst samples	Dry gas (wt%)	Liquefied gas (wt%)	Light fraction oil (wt%)	Heavy cycle oil (wt%)	Coke (wt%)
Cat-1	2.5	15.6	59.2	10.8	11.9
Cat-2	2.4	16.8	55.6	12.1	13.1
Cat-3	2.7	16.1	57.1	11.6	12.5

Table 3 Physicochemical properties of the MYs

Samples	S_{BET} ($m^2\ g^{-1}$)	S_{mic} ($m^2\ g^{-1}$)	S_{meso} ($m^2\ g^{-1}$)	V_{total} ($cm^3\ g^{-1}$)
Cat-1	329	204	125	0.32
Cat-2	278	191	87	0.23
Cat-3	302	197	105	0.29

The BET properties of the three catalysts are listed in Table 3. The high crystallinity (85%) and high mesoporous surface area (133 $m^2 g^{-1}$) of MHY-0.03 gives it better catalytic properties than MHY-*c*.[16] Moreover, the high BET surface area (329 $m^2 g^{-1}$) and high mesoporous surface area (125 $m^2 g^{-1}$) of Cat-1 favor the diffusion of intermediate products. The mechanisms associated with these results need further investigation.

Conclusions

In summary, this investigation has presented a facile route for the synthesis of zeolite Y with intracrystalline mesopores using a greatly reduced amount of organic surfactant. A novel template (TPHAC) with 16 carbon atoms in the hydroxyl chain has been obtained. The content of TPHAC necessary for the formation of integrated micelles decreased greatly due to the decreased number of carbon atoms in the hydroxyl chains. Mesoporous zeolite Y obtained by this route exhibits excellent hydrothermal stability. This investigation resulted in the development of a unique synthesis route to zeolite Y with intracrystalline mesopores and excellent catalytic properties.

Conflict of interest

The authors declare no competing financial interest.

Acknowledgements

The authors acknowledge the financial support from the Natural Science Foundation of China (Grant No. 20606003).

References

1 J. García-Martínez, K. Li and G. Krishnaiah, *Chem. Commun.*, 2012, **48**, 11841–11843.
2 J. Garcíamartínez, M. Johnson, J. Valla, K. Li and J. Y. Ying, *Catal. Sci. Technol.*, 2012, **2**, 987–994.
3 T. F. Degnan, *Top. Catal.*, 2000, **13**, 349–356.
4 Z. Qin, B. Shen, Z. Yu, F. Deng, L. Zhao, S. Zhou, D. Yuan, X. Gao, B. Wang and H. Zhao, *J. Catal.*, 2013, **298**, 102–111.
5 Z. Qin, B. Shen, X. Gao, F. Lin, B. Wang and C. Xu, *J. Catal.*, 2011, **278**, 266–275.
6 W. Fu, L. Zhang, T. Tang, Q. Ke, S. Wang, J. Hu, G. Fang, J. Li and F. S. Xiao, *J. Am. Chem. Soc.*, 2011, **133**, 15346–15349.
7 Z. L. Hua, J. Zhou and J. L. Shi, *Chem. Commun.*, 2011, **47**, 10536–10547.
8 D. Verboekend and J. Pérez-Ramírez, *Catal. Sci. Technol.*, 2011, **1**, 879–890.
9 D. P. Serrano, J. M. Escola and P. Pizarro, *ChemInform*, 2013, **42**, 4004–4035.
10 D. Verboekend, G. Vilé and J. Pérezramírez, *Cryst. Growth Des.*, 2012, **12**, 3123–3132.
11 C. M. Parlett, K. Wilson and A. F. Lee, *Chem. Soc. Rev.*, 2013, **42**, 3876–3893.
12 X. Meng, F. Nawaz and F. S. Xiao, *Nano Today*, 2009, **4**, 292–301.
13 J. Ding, J. Hu, Y. Guan, H. Wu and M. Y. He, *Catal. Commun.*, 2016, **86**, 139–142.
14 P. Peng, Y. Wang, Z. Zhang, K. Qiao, X. Liu, Z. Yan, F. Subhan and S. Komarneni, *Chem. Eng. J.*, 2016, **302**, 323–333.
15 J. R. García, M. Falco and U. Sedran, *Top. Catal.*, 2016, **59**, 268–277.
16 W. Li, J. Zheng, Y. Luo and Z. Da, *Appl. Surf. Sci.*, 2016, **382**, 302–308.
17 H. S. Cho and R. Ryoo, *Microporous Mesoporous Mater.*, 2012, **151**, 107–112.
18 C. Manrique, A. Guzmán, J. Pérez-Pariente, C. Márquez-Álvarez and A. Echavarría, *Fuel*, 2016, **182**, 236–247.
19 M. Choi, H. S. Cho, R. Srivastava, C. Venkatesan, D. H. Choi and R. Ryoo, *Nat. Mater.*, 2006, **5**, 718–723.
20 B. Liu, K. Xie, C. O. Su, D. Sun, Y. Fang and H. Xi, *Chem. Eng. Sci.*, 2016, **153**, 374–381.
21 J. Jin, C. Peng, J. Wang, H. Liu, X. Gao, H. Liu and C. Xu, *Ind. Eng. Chem. Res.*, 2014, **53**, 3406–3411.
22 L. Yu, S. Huang, M. Shu, X. Zhu, S. Zhang, Z. Liu, W. Xin, S. Xie and L. Xu, *Ind. Eng. Chem. Res.*, 2014, **53**, 693–700.
23 K. Na, M. Choi and R. Ryoo, *Microporous Mesoporous Mater.*, 2013, **166**, 3–19.
24 K. Cho, H. S. Cho, L. C. D. Ménorval and R. Ryoo, *Chem. Mater.*, 2009, **21**, 5664–5673.
25 K. Na, W. Park, Y. Seo and R. Ryoo, *Chem. Mater.*, 2011, **23**, 1273–1279.
26 J. Kim, C. Jo, S. Lee and R. Ryoo, *J. Mater. Chem. A*, 2014, **2**, 11905–11912.